Food Sci. Biotechnol. Vol. 17, No. 5, pp. 1038 ~ 1046 (2008)

Food Science and Biotechnology

Development, Validation, and Application of a Portable SPR Biosensor for the Direct Detection of Insecticide Residues

Gilmo Yang* and Nam-Hong Cho

National Institute of Agricultural Engineering, Rural Development Administration, Suwon, Gyeonggi 441-100, Korea

Abstract This study was carried out to develop a small-sized biosensor based on surface plasmon resonance (SPR) for the rapid identification of insecticide residues for food safety. The SPR biosensor module consists of a single 770 nm-light emitting diodes (LED) light source, several optical lenses for transferring light, a hemisphere sensor chip, photo detector, A/D converter, power source, and software for signal processing using a computer. Except for the computer, the size and weight of the sensor module are 150 (L)×70 (W)×120 (H) mm and 828 g, respectively. Validation and application procedures were designed to assess refractive index analysis, affinity properties, sensitivity, linearity, limits of detection, and robustness which includes an analysis of baseline stability and reproducibility of ligand immobilization using carbamate (carbofuran and carbaryl) and organophosphate (cadusafos, ethoprofos, and chlorpyrifos) insecticide residues. With direct binding analysis, insecticide residues were detected at less than the minimum 0.01 ppm and analyzed in less than 100 sec with a good linear relationship. Based on these results, we find that the binding interaction with active target groups in enzymes using the miniaturized SPR biosensor could detect low concentrations which satisfy the maximum residue limits for pesticide tolerance in Korea, Japan, and the USA.

Keywords: surface plasmon resonance, biosensor, insecticide, pesticide, carbamate, organophosphate

Introduction

An insecticide is a pesticide used against insects of all developmental forms. They include ovicides and larvicides used against the eggs and larvae of insects. All pesticides are poisons. There are hundreds of pesticide products from which to choose. They are designed to kill or repel pests but may be harmful and/or fatal to other organisms, including humans. Pesticides contribute significantly to overall cancer mortality (1-3).

During 2005, the pesticide data program (PDP) of the United States Department of Agriculture (USDA) tested fresh and processed fruit, vegetables, pork, bottled water, and drinking water for various insecticides, herbicides, fungicides, and growth regulators. Of the 14,749 total samples collected and analyzed, 10,154 were fruit and vegetable commodities, of which 8,702 were fresh products and 1,452 were processed products. They were collected by each of the 10 sampling states (California, Colorado, Florida, Maryland, Michigan, New York, Ohio, Texas, Washington, and Wisconsin). Overall, 73% of fresh fruit and vegetables, and 61% of processed fruit and vegetables showed detectable residues. More residues were detected in fresh produce than in processed products and grains. Residues exceeding tolerance levels were also detected in 0.2% of the 13,621 samples (4).

Food and agricultural production facilities and regulatory inspectors need sensitive and accurate tests for the detection of pesticide residues in food and on food processing surfaces. Rapid tests are essential to allow the detection of contaminated foods before they are distributed to consumers. The analysis of insecticides is usually carried out by gas and liquid chromatography with a selective-element detector (5). These procedures frequently require laborious extraction and clean-up steps that increase the risk of sample loss, are time consuming and constitute the primary source of errors and discrepancies between laboratories (6).

An analytical method using a biosensor represents one of the most promising methods for overcoming such problems (7). In recent years, numerous biosensing methods for the detection of pesticides have been developed using enzyme-based and affinity-based sensors as well as several types of transducers. The enzymatic determination of pesticides is most often based on inhibition. A number of different biosensors have been constructed using acetylcholinesterase (AChE) (8-11), glutathione-*S*-transferase (GST) (12-14), and goat anti-rabbit IgG peroxidase conjugate (IgG) (15-19) with modified electrochemical (8,10,11,20), photothermal (21), fiber optic transducers (16,22), and biomarker transducers (23-25). Whole cells such as *Chlorella vulgais* microalgae and *Flavobacterium* sp. as bioreceptors have also been used as a bi-enzymatic biosensors (26,27). Biosensors using these transducers based on enzyme inhibition, although sensitive, have a limitation: the linearity between the concentration of the object pesticide and the measured amount of signal are not sufficient for economic practicality. Also, low repeatability has been reported for assays of whole-cell bacterial biosensors by their physical characteristics (28).

A surface plasmon resonance (SPR) system has been reported to be an effective transducer for biosensors because the SPR system was originally developed for studying the interactions of biomolecules such as proteins and DNA. This is due to the fact that the SPR system is a highly sensitive real-time automated monitoring device and would be suitable for detecting the target analytes without the pretreatment of samples. Thus an analytical method based

*Corresponding author: Tel: +82-31-290-1916; Fax: +82-31-293-9752
E-mail: okmomo@gmail.com
Received February 27; Revised April 18, 2008;
Accepted April 24, 2008

on an SPR system might be useful for the sensitive detection of pesticides and related compounds (7,29-32).

Therefore, the objective of this work was to develop a rapid, small, and inexpensive SPR biosensor module to meet these requirements (14,19). Validation and application procedures were designed to assess refractive index analysis, affinity properties, sensitivity, linearity, detection limits, and robustness, which includes an analysis of baseline stability and reproducibility of ligand immobilization using organophosphorous and carbamate insecticides diluted in water.

Materials and Methods

Materials Standard carbamate (carbofuran, carbaryl) and organophosphate (cadusafos, ethoprofos, chlorpyrifos) pesticides, peroxidase conjugated to goat anti-rabbit IgG (whole molecule), phosphate-buffered physiological saline (PBS, 10 mM, pH 7.4), 10 mM HEPES-NaOH (pH 7.4) and 11-mercaptoundecanoic acid (11-MUA) were purchased from Sigma-Aldrich (St. Louis, MO, USA). Working standard solutions were prepared daily by dilution in PBS-Tween (10 mM PBS with 18 MΩ distilled water) for reacting to antibody. One M ethanolamine (pH 8.5, Biacore AB, Uppsala, Sweden) was used for stabilizing chip surfaces. Common chemicals used in sensor surface immobilization were also purchased from Sigma-Aldrich: 100 mM *N*-hydroxysuccinimide (NHS), and 400 mM *N*-ethyl-*N*'-(3-dimethylamino-propyl) carbodiimide hydrochloride (EDC). PBS buffer was filtered through a 0.2-μm membrane filter and degassed.

IgG antibody was isolated from goat anti-rabbit IgG antiserum by immunospecific purification that removed essentially all goat serum proteins, including immunoglobulins that do not specifically bind to rabbit IgG. Goat anti-rabbit antibody was conjugated to horseradish peroxidase (HRP). Antibody fabrication and the affinity purification of IgG have been described by a modification of the periodate method of Wilson and Mouvet (33,34).

The SPR sensor module basically consisted of a 770 nm-light emitting diodes (LED) (770 LED module; Roithner-Laser Technik, Inc., Vienna, Austria) light source (35), several optical lenses for transferring light, a hemisphere sensor chip, light-division mirrors, photo detector, amplifier, A/D converter, power source, and computer for signal processing as shown in Fig. 1A. It was developed based on Kretschman's geometry theory (29) concept of Spreeta sensors (Texas Instruments, Dallas, TX, USA), Nakajima's SPR sensor (31) and Biacore 3000 equipment (Biacore AB). LED light from the light source illuminates the gold-coated glass surface with SPR angles after passing through a polarizing filter and cylindrical lens, which selects light for decreasing reflection from sensor chip surface and bends light in only one direction. After reflection from the gold-coated chip surface, the light is directed towards the linear photo detector (TH7814A; Atmel Co., San Jose, CA, USA) with the help of lenses and mirrors. The response of the photo detector is amplified and digitized by an A/D converter and then transferred to a computer. The developed monitoring and analysis program provides the user with the sensor data for displaying and analyzing an SPR curve. Except for the computer, the size and weight of the sensor were designed to be 150 (L)×70 (W)×120 (H) mm and 828 g, respectively (Fig. 1B).

The gold coated hemisphere sensor chip with prism consisted of a BK7 Plano-convex cylindrical lens (Red Optronics Co. Mountain View, CA, USA), a 17×17 mm sized cover glass with 50 nm gold layer and a silicone rubber gasket 3 mm thick and 6 mm in diameter with 2 ports, a basis port and sample port (Fig. 1C). The volume of each port is about 85 μL. A pipette was used to inject samples on the chip surface.

Immobilization of IgG on gold chip surface Layer-by-layer (LBL) and amine coupling procedures were used for forming a self-assembled layer on the Au chip surface (36, 37). Bare gold substrate for the basis and sample ports was immersed into an 11-MUA in ethanol for 16 hr, and then rinsed with absolute ethanol and deionized water before drying with 99.999% nitrogen (38). Following the activation of the sensor chip surface with 400 mM EDC and 100 mM NHS, 0.1 mg/mL IgG antibody was injected and coupled to the activated surfaces by its free amines. The excess antibodies were removed by rinsing with PBS, and then the antibody-modified SPR chip surface was treated with 1 M ethanolamine, pH 8.5, to remove the non-covalently bound protein conjugate and to block all unreacted NHS-esters remaining on the sensor surface. The schematic diagram for sensor activation and enzyme binding is shown in Fig. 2.

Enzymatic assays Immunochemical analysis is based upon the specific reaction between IgG antibody and its corresponding pesticide. Antibodies are part of the vertebrate defense system (39,40). They are serum glycoproteins of the Ig class produced by the immune system against pesticides, and bind the target substance with high selectivity and affinity. The binding is a result of π-π electron interactions and van der Waals forces. The binding energy relates to the number of specific chemical interactions between the pesticides and the amino acid residues in the IgG combining site (41). In bioaffinity recognition, the binding is very strong, and the SPR transducer detects the presence of the bound antibody-antigen pairs. Therefore, the selectivity and sensitivity of an immunochemical assay is controlled by the nature of the IgG-pesticide binding process and the performance of SPR transducer.

Six-fold serially-diluted pesticides were introduced, starting with the lowest concentration (0.001 ppm) and progressing to the highest concentration (100 ppm), to determine sensitivity, linear regression, detection limits, reproducibility, stability, and reaction times. The target analytes tested for reacting with enzyme were 2 carbamate (carbofuran, carbaryl) and 3 organophosphate (cadusafos, ethoprofos, chlorpyrifos) compounds which have been frequently exposed to the pesticide data program of the National Agricultural Products Quality Management Service (NAQS) in Korea and the USDA from 2005 to 2006 (4,42). The serial dilutions were made in PBS buffer to reduce bulk effects. Sample injections into the SPR system were done by pipette. After sample injection, running buffer was injected on the sensor surfaces followed by 10 mM NaOH washes for regeneration in between each concentration to remove remaining bound pesticide analyte

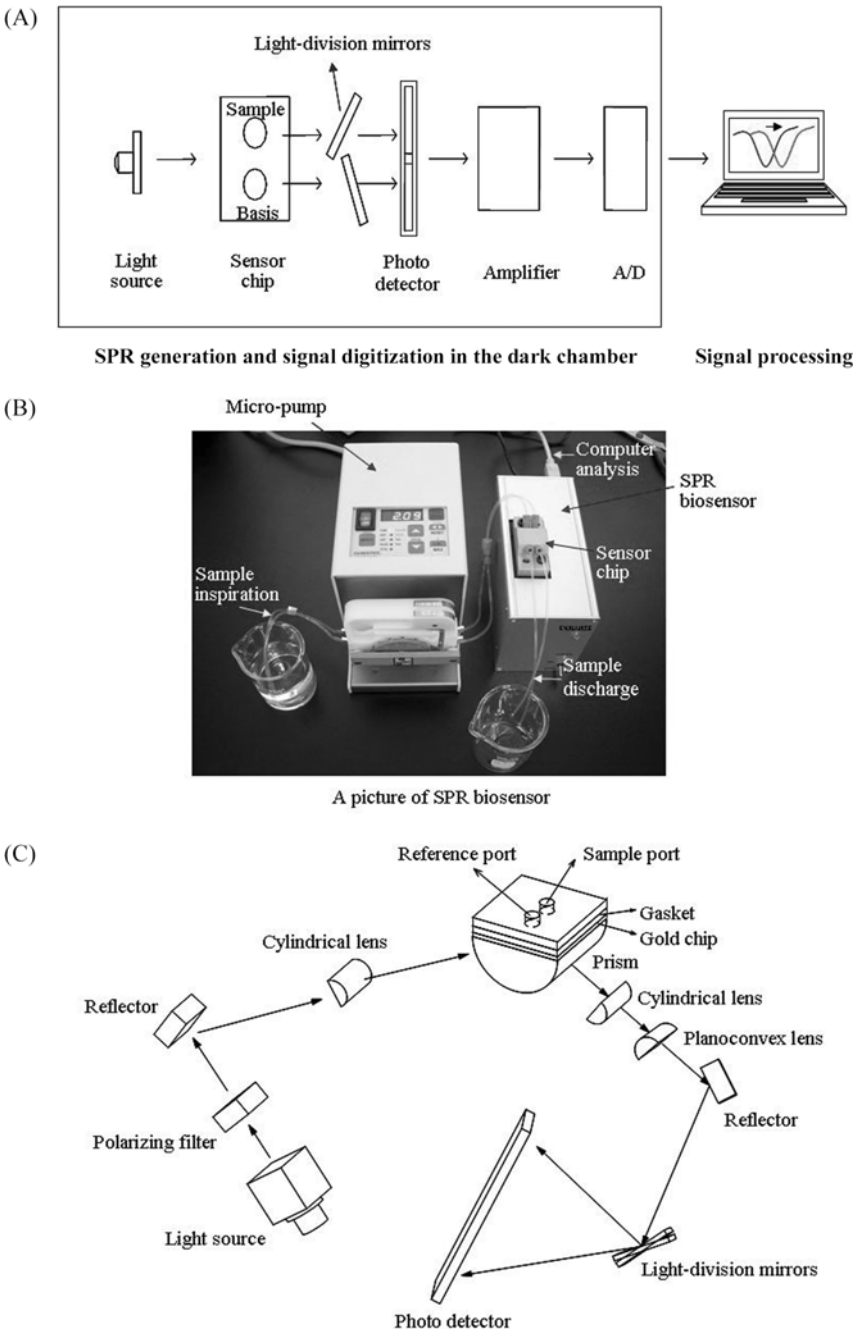

Fig. 1. Constitution of the sensing system: (A) schematic of overall sensor line up, (B) picture of the SPR biosensor, and (C) optical system for SPR generation. Dark chamber includes the optical arrangement which is generating the SPR phenomenon and signal digitization. SPR signal is transmitted to computer for data analysis.

from immobilized IgG ligand. To determine the effect of pH on enzyme activities, experiments were carried out using different sodium acetate buffers (pH 7.0-3.0). The relationship between refractive index and the concentration of the ethanol-water mixture was also determined for the calibration curve. All experiments were carried out at 24°C.

Interaction kinetic data corresponding to different concentrations of analytes were fitted to provide information on the rates of the interaction using the GraphPad Prism 5 (GraphPad Software, Inc., San Diego, CA, USA) and Microsoft Excel 2003 (Microsoft Corp., Redmond, WA, USA) computer software. Determination of the mean values of replicates, standard deviations, and the coefficients of variation was also achieved by triplicate experiments.

The interaction analysis was performed with several binding models for numerical integration and global analysis, including a simple one-to-one binding model (Langmuir) and a homogeneous interaction model with mass transport effects (43). The association rate constant (k_a) and dissociation rate constant (k_d) for the formation of the complex are described by the equations below:

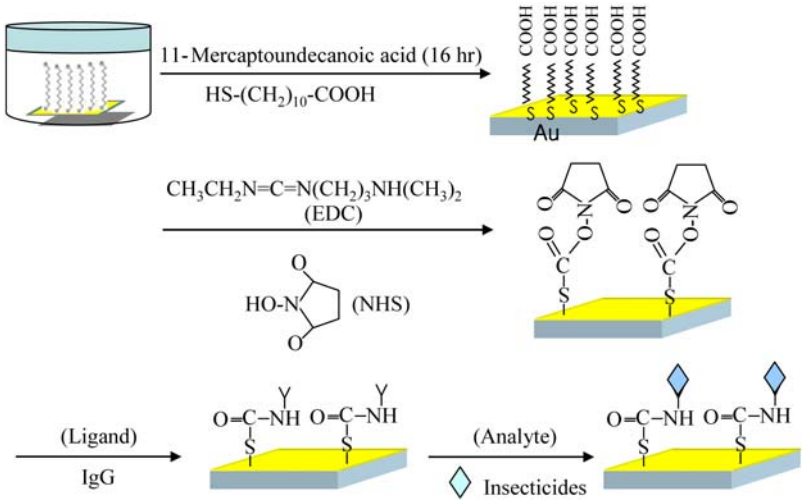

Fig. 2. Schematic diagram for sensor activation and enzyme binding. Sensor chip surface was activated by MUA and EDC/NHS and then ligand was immobilized.

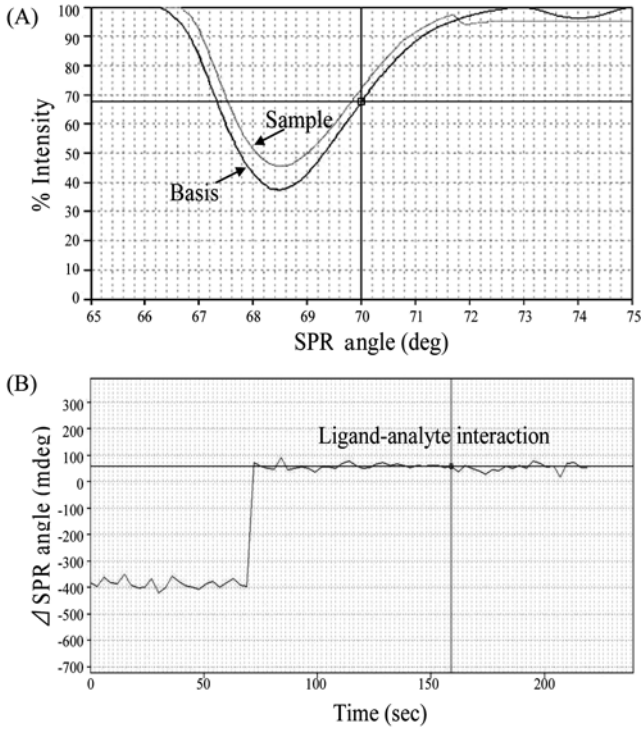

Fig. 3. Pictures of SPR sensograms for carbofuran analyte: (A) SPR intensity shift and (B) resonance angle difference induced by ligand and analyte interaction. SPR intensity was increased by antibody-antigen reaction. And then, SPR angle was shifted as much as several hundred mdeg. After the reaction, the sensor chip was washed with 10 mM NaOH.

$$A+B \xrightarrow{k_a} AB \text{ (1/M/sec)} \quad (1)$$

$$AB \xrightarrow{k_d} A+B \text{ (1/sec)} \quad (2)$$

$$dAB/dt=(k_a \times A \times B - k_d \times AB) \quad (3)$$

where A represents the concentration of analyte in the solution, B represents the ligand immobilized on the sensor surface, and AB is the complex formed by A and B. The association phase was evaluated without knowledge of k_d by using the model 1:1 (Langmuir) association (kobs) (44).

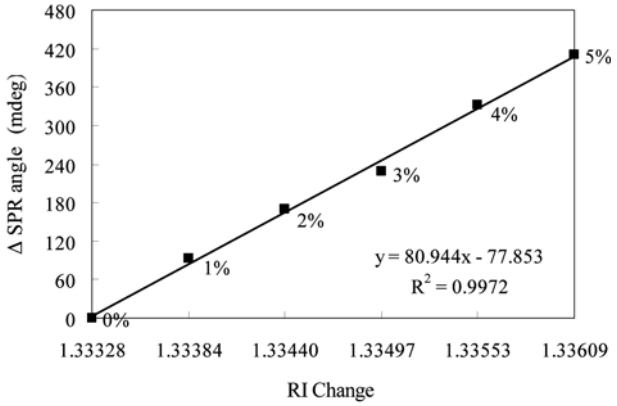

Fig. 4. Refractive index test using ethanol. Samples from 0 to 5% ethanol in water were prepared.

The association equilibrium constant (K_A) was also calculated based on the ratio of k_a/k_d as shown in the following equation:

$$K_A = \frac{k_a}{k_d} = \frac{[AB]}{[A][B]} = \frac{1}{K_D} \quad (4)$$

Masuda *et al.* (45) suggested the complex formation in a binary association as follows:

$$\frac{dR}{dt} = k_a C R_{max} - (k_a C + k_d) R \quad (5)$$

where dR/dt is the rate of change of the SPR signal reflecting the amount of analyte bound to the immobilized ligand on the sensor chip, C is the concentration of analyte, R_{max} is the maximal binding capacity of analyte in resonance unit (RU) when the binding sites of the immobilized ligand have been saturated by the analyte, and R is the SPR signal in RU at time t.

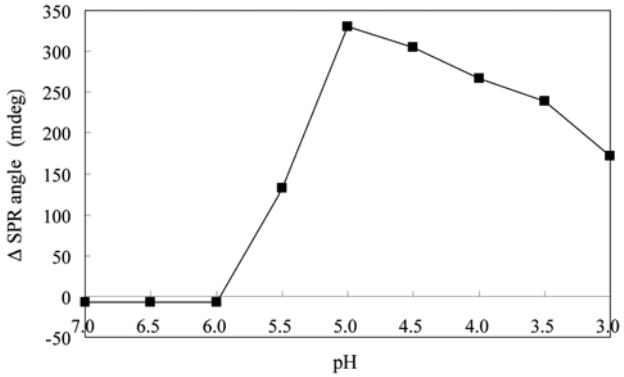

Fig. 5. Effect of buffer pH on binding affinity and enzyme activities. Binding condition analysis was performed from pH 7.0 to pH 3.0.

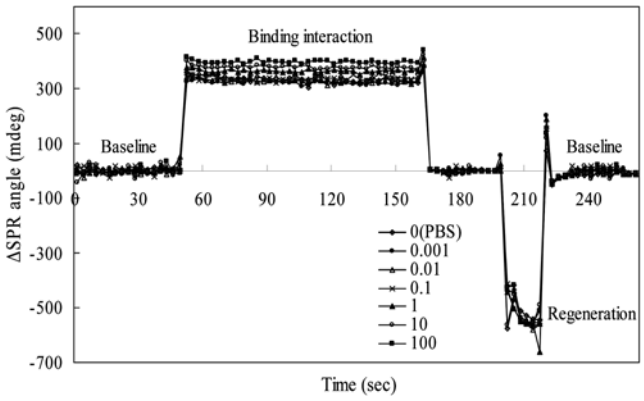

Fig. 6. An example of kinetic analysis data by dilution. sensograms generated by the injection of 6 distinct concentrations of carbofuran analyte.

Results and Discussion

SPR sensograms The SPR sensor chip consisted of a basis port and a sample port. Figure 3 shows the monitoring sensogram screen with resonance signals of the SPR responses obtained in a non-modified basis port filled with PBS buffer and the IgG-pesticide interactions in the sample port. The resonance angle gained from the sample port was shifted to a higher angle by 0.055° compared to the basis port when the sensor chip coated by IgG ligand was exposed to pesticide analyte as illustrated in Fig. 3B. This angle shift means that 0.055 ng/mm^2 mass transformation was generated by the alteration of enzymatic activity, which resulted in the change of interaction with its substrate.

Bulk refractive index analysis The SPR sensor calibration curve was characterized by bulk refractive index (RI) change, as shown in Fig. 4, because the sensing mechanism of the SPR biosensor is based on RI detection. Various water-ethanol mixtures from 0 to 5% with known RI were injected sequentially on the bare gold chip surface. A good linear relationship between SPR intensity and RI change using ethanol was obtained. After the RI analysis, the chip surface was rinsed with 18 MΩ water and filled with PBS buffer for chip activation.

Determination of binding conditions The effect of buffer pH on enzyme activity is illustrated in Fig. 5. The IgG enzymes diluted in different sodium acetate buffer solutions ranging from pH 7.0 to 3.0 were injected serially. The results indicate that the optimal pH for IgG immobilization on the chip surface is 5.0. This means that the electrostatic attraction between negative charges on the gold chip surface and positive charges on the IgG enzyme at pH 5.0 was higher than the previous pH values for covalent linking. So we chose a pH value of 5.0 to immobilize IgG enzyme on the gold chip surface.

Affinity properties of insecticide-IgG conjugates Figure 6 shows 6 sets of kinetic analysis data. The kinetic curves were adequately fitted to the Langmuir model and provide

Table 1. Kinetic and affinity data from the SPR analysis of insecticides

Insecticide	Kinetic parameter	Concentration (ppm, μg/mL)					
		0.001	0.01	0.1	1	10	100
Carbofuran	k_a (1/M/min)	1.68×10^{8}	1.77×10^{8}	1.63×10^{8}	1.72×10^{8}	1.74×10^{8}	1.72×10^{8}
	k_d (1/min)	6.72×10^{-1}	6.77×10^{-1}	6.05×10^{-1}	6.49×10^{-1}	6.72×10^{-1}	6.50×10^{-1}
	K_A (1/M)	2.50×10^{8}	2.61×10^{8}	2.69×10^{8}	2.66×10^{8}	2.60×10^{8}	2.65×10^{8}
Carbaryl	k_a (1/M/min)	2.68×10^{8}	2.66×10^{8}	2.41×10^{8}	2.65×10^{8}	2.78×10^{8}	2.62×10^{8}
	k_d (1/min)	2.15×10^{0}	2.32×10^{0}	1.95×10^{0}	2.30×10^{0}	2.31×10^{0}	2.36×10^{0}
	K_A (1/M)	1.25×10^{8}	1.15×10^{8}	1.24×10^{8}	1.15×10^{8}	1.20×10^{8}	1.11×10^{8}
Cadusafos	k_a (1/M/min)	1.02×10^{8}	9.36×10^{7}	1.12×10^{8}	1.28×10^{8}	1.06×10^{8}	1.12×10^{8}
	k_d (1/min)	5.48×10^{-1}	5.78×10^{-1}	5.32×10^{-1}	4.75×10^{-1}	5.44×10^{-1}	5.22×10^{-1}
	K_A (1/M)	1.87×10^{8}	1.62×10^{8}	2.11×10^{8}	2.70×10^{8}	1.94×10^{8}	2.15×10^{8}
Ethoprofos	k_a (1/M/min)	1.22×10^{8}	1.17×10^{7}	1.18×10^{8}	1.19×10^{8}	1.22×10^{8}	1.19×10^{8}
	k_d (1/min)	1.72×10^{-1}	1.25×10^{-1}	1.07×10^{-1}	1.13×10^{-1}	1.16×10^{-1}	1.05×10^{-1}
	K_A (1/M)	7.10×10^{8}	9.41×10^{8}	1.11×10^{9}	1.06×10^{9}	1.05×10^{9}	1.12×10^{9}
Chrorpyrifos	k_a (1/M/min)	1.57×10^{8}	1.53×10^{7}	1.60×10^{8}	1.59×10^{8}	1.57×10^{8}	1.57×10^{8}
	k_d (1/min)	5.27×10^{-1}	5.34×10^{-1}	5.51×10^{-1}	5.59×10^{-1}	5.40×10^{-1}	5.14×10^{-1}
	K_A (1/M)	2.99×10^{8}	2.86×10^{8}	2.90×10^{8}	2.84×10^{8}	2.91×10^{8}	3.06×10^{8}

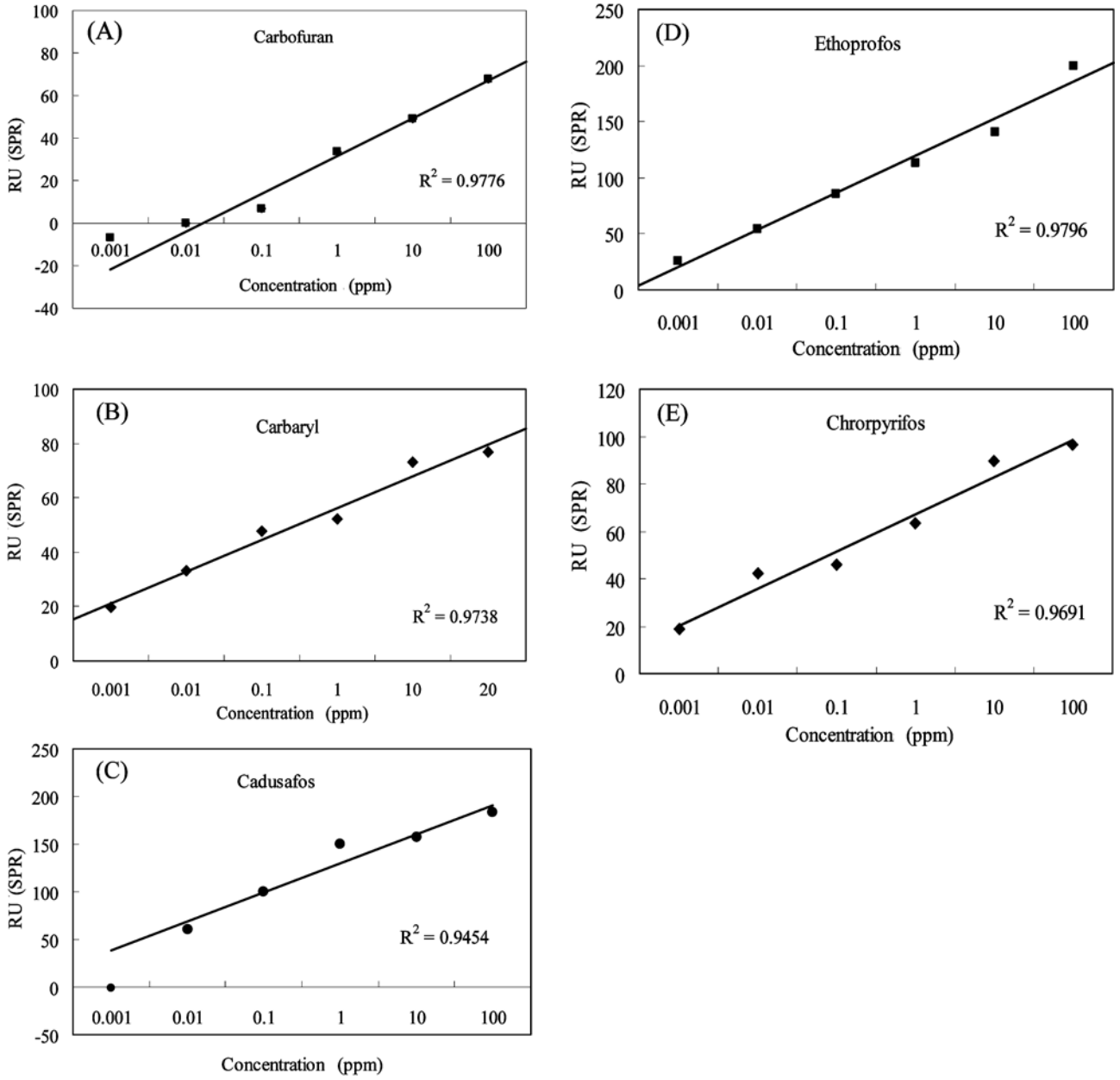

Fig. 7. Direct binding assay between IgG ligand and insecticides. (A) Carbofuran and (B) carbaryl are carbamate insecticides, (C) cadusafos, (D) ethoprophos, and (E) chrorpyrifos are organophosphate insecticides. Measurements were carried out in triplicate.

sufficient information about affinity properties between IgG enzyme and insecticide analytes. Several analyte injections generated binding profiles with distinct curvatures during the association phase. The sensograms were almost straight during injection, with little or no curvature even when binding approached saturation levels. This indicates that the sensograms mainly reflect steady-state levels at saturation. Dissociation events using a pipette occurred faster than the time it usually took to use a peristaltic pump or a syringe pump.

Corresponding to a χ^2 value lower than 1, the kinetic parameters obtained are shown in Table 1. These sensograms were also fitted locally to the same kinetic model. The saturation binding experiments were also plotted against the concentration of insecticide residues so that the affinity constant (K_A) values derived from this plot and calculated by the ratio could be compared. With the experimental design and kinetic analysis model described here, it could be possible to determine the binding rate constants in the following ranges: $k_a=10^7–10^8$/M/min, $k_d=10^{-1}–10^0$ and $K_A=10^8–10^9$.

Affinity is not the ideal parameter, however this shows that kinetic data directly links a change in structure to changes in recognition (k_a), stability (k_d), or both information that can improve the lead to optimization of the procedure (46,47).

Evaluation of measurement sensitivity, linearity, and detection limit The measurement sensitivity of the SPR biosensor, the surface of which was modified with the IgG

ligand, was examined for 2 kinds of carbamate (carbofuran and carbaryl) and 3 kinds of organophosphate (cadusafos, ethoprofos, and chrorpyrifos) (19) insecticides by introducing 85 μL of 0.001-100 ppm sample solutions into the SPR system as shown in Fig. 7.

The PBS buffer response was subtracted from the active surface (IgG) response to insecticide analytes when direct binding analysis of the SPR response and the range of analyte concentrations was carried out. This differential SPR intensity was expressed in RU. Therefore, the resulting values in minus RU for each concentration level suggest that this SPR biosensor could not provide enough sensitivity for the detection of that level of sample. The RU values of the samples increased with increasing insecticide concentrations in the immersing solution. Under the same experimental conditions, ligand-analyte interactions exhibited a good linear relationship between the amount of bound material and the shift of the SPR angle with the correlation coefficients from a minimum of 0.9454 for cadusafos to a maximum of 0.9796 for ethoprofos.

The SPR's performance is restricted by the size (angular change, wavelength, and intensity modulation) (35,48,49), the distribution of Au nanoparticles (49) and the signal/noise ratio that is defined by the system's electronic components (50). This restricted the system's resolution for sensitivity and detection limits at low concentrations. However, the sensing configuration of the small SPR biosensor resulted in a linear dependence of the sensor response on the refractive index of the sample medium at high concentration, without reaching the saturation point (50,51).

The limits of detection (LODs) followed by linear sections were measured to be 0.01 ppm for carbofuran and cadusafos, and 0.001 ppm for carbaryl, ethoprofos, and chrorpyrifos. The binding interaction with active target groups in the enzyme could reach low concentrations which satisfied the maximum residue limits (MRLs); 0.01 ppm, for pesticide tolerance in Korea, Japan, and the USA (Table 2) (4, 52, 53). However, although this portable SPR biosensor has enough function for quantitative analysis using polyclonal antibody, qualitative analysis using monoclonal antibody for multicomponent pesticide residues is insufficient for a 2-channel sensor signal processor. Thus, in considering future research toward this

Table 2. Regressions of each composition from 0.001 to 100 ppm

Insecticide	Regressions line	Correlation coefficients (R^2)	Limits of detection (LOD) (ppm, μg/mL)	Maximum residue limit (MRL) (ppm, μg/mL)
Carbofuran	y=17.83x-39.82	0.978	0.01	0.01-2
Carbaryl	y=11.67x+9.56	0.974	0.001	0.2-3
Cadusafos	y=30.29x+8.76	0.945	0.01	0.01-0.2
Ethoprofos	y=33.03x-12.49	0.980	0.001	0.005-0.02
Chrorpyrifos	y=15.64x+4.68	0.969	0.001	0.05-0.5

Table 3. Statistical data for insecticide residues by triplicate experiments[1)]

Conc. (ppm)	Carbofuran				Carbaryl (Max 20 ppm)				Cadusafos				Ethoprofos				Chrorpyrifos			
	RU (n=3)	AVG	SD	%CV	RU (n=3)	AVG	SD	%CV	RU (n=3)	AVG	SD	%CV	RU (n=3)	AVG	SD	%CV	RU (n=3)	AVG	SD	%CV
0.001	309 331 330	323	12.6	3.9	118 123 121	121	2.2	1.8	303 351 340	331	24.9	7.5	159 184 169	171	12.6	7.4	184 189 204	193	10.3	5.3
0.01	330 322 340	331	9.3	2.8	144 110 147	134	20.5	15.3	400 388 389	392	6.6	1.7	213 209 177	200	19.4	9.7	223 213 211	216	6.7	3.1
0.1	357 319 335	337	19.0	5.6	146 138 162	149	11.9	8.0	423 452 419	431	18.2	4.2	229 245 216	230	14.3	6.2	234 219 204	219	15.2	6.9
1	340 393 369	367	26.8	7.3	168 143 150	153	12.7	8.3	481 476 487	481	5.1	1.1	279 250 245	258	18.4	7.1	240 253 219	237	17.0	7.2
10	400 395 355	383	24.5	6.4	179 168 175	174	5.5	3.2	501 478 490	490	11.7	2.4	290 286 282	286	3.9	1.4	256 253 279	263	14.3	5.5
100 (20)	378 410 406	398	17.3	4.3	170 173 190	178	11.0	6.2	494 538 516	516	22.3	4.3	357 313 363	344	27.7	8.0	292 266 252	270	20.1	7.4
0 (PBS)	334 328 328	330	3.6	1.1	102 100 101	101	0.7	0.7	339 330 326	332	6.9	2.1	141 145 148	145	3.2	2.2	173 174 174	174	0.6	0.4

[1)]SD, standard deviation; CV, coefficient of variation.

end, the deficiency could be settled by the development of multichannel sensing technology.

Sensitivity, linearity, LODs, and robustness were examined in detail using the binding interaction with active target groups in the enzyme. This sensor module could be configured as a portable, handheld device for use on farms and in processing plants, providing researchers and regulators with an important tool for controlling food contamination.

Reproducibility and stability The reproducibility of the present sensor based on 5 random sample injections was investigated. As a result, the coefficients of variation (CV) of RU values for each analyte were distributed from a minimum of 3.5% for cadusafos to a maximum of 7.1% for carbaryl based on the mean of triplicate experiments as shown in Table 3. The high CV distributions of carbaryl samples were thought to be due to the manual injection of samples using pipettes as opposed to using a micro pump with a constant flow rate. This caused the base line to be a little bit unstable when the samples were injected. This suggests that we should devise an apparatus to keep a constant flow rate and achieve sensor stability.

The reaction time was defined as the time from sample injection to the beginning of the ligand-analyte interaction, measured in less than 100 sec (Fig. 3B). This shows that a real-time detection, monitoring, and affinity study in solution with a binding partner immobilized on the surface of the sensor would be possible with the present SPR biosensor.

Further experiments addressing SPR biosensor applications in the detection of insecticide residues on actual spiked food is required, such as the testing of rinsed samples. Also, we should install a device for sample injection on the chip surface to improve sensor stability. Ultimately, a standard curve of this SPR biosensor applied to the detection of insecticide residues on real water extracted from agricultural and food products should be obtained for commercial applications. The qualitative and quantitative analysis for detecting pesticide residues can be enhanced by improving the bioreceptor on the SPR sensor platform.

Acknowledgments

This research was supported by the National Institute of Agricultural Engineering, Rural Development Administration, Korea.

References

1. Len R. Report of a panel on the relationship between public exposure to pesticides and cancer. Cancer 80: 1887-1888 (1997)
2. Chun MH, Lee MG. Reduction of pesticide residues in the production of red pepper powder. Food Sci. Biotechnol. 15: 57-62 (2006)
3. Kang SM, Lee MG. Fate of some pesticides during brining and cooking of Chinese cabbage and spinach. Food Sci. Biotechnol. 14: 77-81 (2005)
4. USDA. Annual Summary for Pesticide Data Program. United States Department of Agriculture (USDA), Washington DC, USA. pp. 4-5 (2005)
5. Nunes S, Skladal P, Yamanka H, Barcelo D. Determination of carbamate residues in crop samples by cholinesterase-based on biosensors and chromatographic techniques. Anal. Chim. Acta 362: 59-68 (1998)
6. Ni Y, Qiu P, Kokot S. Simultaneous viltammetric determination of four carbamate pesticides with the use of chemometrics. Anal. Chim. Acta 537: 321-330 (2005)
7. Nobuaki S, Tomoyuki T, Tomomi W, Keiko M, Toshihiko I, Takashi M, Yasukazu A, Saeko O, Osamu N, Stanley B. A surface plasmon resonance immunosensor for detecting a dioxin precursor using a gold binding polypeptide. Talanta 60: 733-745 (2003)
8. Kok FN, Hasirci V. Determination of binary pesticide mixtures by an acetylcholinesterase-choline oxidase biosensor. Biosens. Bioelectron. 19: 661-665 (2004)
9. Suwansa-ard S, Kanatharana P, Asawatreratanakul P, Limsakul C, Wongkittisuksa B, Thavarungkul P. Semi disposable reactor biosensors for detecting carbamate pesticides in water. Biosens. Bioelectron. 21: 445-454 (2005)
10. Vakurov A, Simpson CE, Daly CL, Gibson TD, Millner PA. Acetylcholinesterase-based biosensor electrodes for organophosphate pesticide detection. Biosens. Bioelectron. 20: 1118-1125 (2004)
11. Vakurov A, Simpson CE, Daly CL, Gibson TD, Millner PA. Acetylcholinesterase-based biosensor electrodes for organophosphate pesticide detection. II Immobilization and stabilization of acetylecholinesterase. Biosens. Bioelectron. 20: 2324-2329 (2005)
12. Andreou VG, Clonis YD. Novel fiber-optic biosensor based on immobilized glutathione *S*-transferase and sol-gel entrapped bromcresol green for the determination of atrazine. Anal. Chim. Acta 460: 151-161 (2002)
13. Choi JW, Lee WH. The development of fiber-optic biosensor for simultaneous detection of the pesticide residues in agricultural products. Agr. Res. Pro. Cent. Korea. pp. 68-83 (2002)
14. Yang GM, Kang SW. SPR-based antibody-antigen interaction study for real time analysis of carbamate pesticide residues. Food Sci. Biotechnol. 17: 15-19 (2008)
15. Dzantiev BB, Yazynina EV, Zherdev AV, Plekhanova YV, Reshetilov AN, Changc SC, McNeil CJ. Determination of the herbicide chlorsulfuron by amperometric sensor based on separation-free bienzyme immunoassay. Sensor Actuat. B-Chem. 98: 254-261 (2004)
16. Harris RD, Luff BJ, Wilkinson JS, Piehler J, Brecht A, Gauglitz G, Abuknesha RA. Integrated optical surface plasmon resonance immunoprobe for simazine detection. Biosens. Bioelectron. 14: 377-386 (1999)
17. Song SJ, Cho HK. Enzyme immunoassay for on-line sensing of the insecticide imidaclopird residues. J. Korean Soc. Agric. Mach. 28: 505-510 (2003)
18. Xing WL, Ma LR, Jiang ZH, Cao FH, Jia MH. Portable fiber-optic immunosensor for detection of methsulfuron methyl. Talanta 52: 879-883 (2000)
19. Yang GM, Kang SW. Detection of multi-class pesticide residues using surface plasmon resonance based on polyclonal antibody. Food Sci. Biotechnol. 17: 547-552 (2008)
20. Brasil PR, Nunes GS, Rodrigues TC, Andreescu S, Marty JL. Comparative investigation between acetycholinesterase obtained from commercial soures and genetically modified drosophila melanogaster application in amperometric biosensors for methaidophos pesticide detection. Biosens. Bioelectron. 20: 825-832 (2004)
21. Pogaènik L, Franko M. Detection of organophosphate and carbamate pesticides in vegetable samples by a photothermal biosensor. Biosens. Bioelectron. 18: 1-9 (2003)
22. Maria PX, Begona V, Maria DM, Maira CM, Baldini AF. Fiber optic monitoring of carbamate pesticides using galss with covalently bound chlorophenol red. Biosens. Bioelectron. 14: 895-905 (2000)
23. Cho H, Yoo S, Kong K. Cloning of a rice tau class GST isozyme and characterization of its substrate specificity. Pestic. Biochem. Phys. 86: 110-115 (2006)
24. Olawale O, Ikechukwu O. Glutathione *S*-transferase (GST) activity as a biomarker in ecological risk assessment of pesticide contaminated environment. Afr. J. Biotechnol. 6: 1455-1459 (2007)
25. Razak CA, Salam F, Ampon K, Basri M, Salleh AB. Development of an ELISA for detection of parathion, carbofuran, and 2,4-dchlorophenoxyacetic aid in water, soil, vegetables, and fruits. Ann. NY Acad. Sci. 864: 479-484 (1998)
26. Chouteau C, Dzyadevych S, Durrieu C, Chovelon JM. A bi-

enzymatic whole cell conductometric biosensor for heavy metal ions and pesticides detection in water samples. Biosens. Bioelectron. 20: 273-281 (2005)
27. Kumar J, Jha SK, D'souza SF. Optical microbial biosensor for detection of methyl parathion pesticide using *Flavobacterium* sp. whole cells adsorbed on glass fiber filters as disposale biocomponent. Biosens. Bioelectron. 21: 2100-2105 (2006)
28. Marinella F, Damià B. Characterization of wastewater toxicity by means of a whole-cell bacterial biosensor, using *Pseudomonas putida*, in conjunction with chemical analysis. Fresen. J. Anal. Chem. 371: 467-473 (2001)
29. Kretschmann E, Reather H. Radiative decay of non-radiative surface plasmons excited by light. Z. Naturforsch. 23: 2135-2136 (1968)
30. Mauriz E, Calle A, Manclús JJ, Montoya A, Escuela AM, Sendra JR, Lechuga LM. Single and multi-analyte surface plasmon resonance assays for simultaneous detection of cholinesterase inhibiting pesticides. Sensor Actuat. B-Chem. 118: 399-407 (2006)
31. Nakajima H, Harada Y, Aanno Y, Nakagama T, Uchiyama K, Imato T, Soh N, Hemmi A. Development of palm-sized differential plasmon resonance meter based on concept of prode. Sensor Actuat. B-Chem. 108: 893-898 (2005)
32. Rajan SC, Gupta BD. Surface plasmon resonance based fiber-optic sensor for the detection of pesticide. Sensor Actuat. B-Chem. 123: 661-666 (2007)
33. Wilson M, Nakane P. Immunofluorescence and Related Staining Techniques. Elsevier/North Holland BioMedical Press, Amsterdam, Netherlands. p. 215 (1978)
34. Mouvet C, Amalric L, Broussard S, Lang G, Brecht A, Gauglitz G. Reflectometric interference spectroscopy for the determination of atrazine in natural water samples. Environ. Sci. Technol. 30: 1846-1851 (1996)
35. Hemmia A, Imato T, Aoki Y, Sato M, Soh N, Asano Y, Akasaka C, Okutani S, Ohkubo S, Kaneki N, Shimada K, Eguchi T, Oinuma T. Development of palm-sized differential plasmon resonance meter based on concept of Sprode. Sensor Actuat. B-Chem. 108: 893-898 (2005)
36. Decher G. Buildup of ultrathin multilayer films by a self-assembly process: III. Consecutively alternating adsorption of anionic and cationic polyelectrolytes on charged surfaces. Thin Solid Films 210-211: 831-835 (1992)
37. Johnsson B, Lofas S, Lindquist G. Immobilization of proteins to a carboxymethyldextran-modified gold surface for biospecific interaction analysis in surface plasmon resonance sensors. Anal. Biochem. 198: 268-277 (1991)
38. Higashi N, Takahashi M, Niwa M. Immobilization of DNA through intercalation at self-assembled monolayers on gold. Langmuir 15: 111-115 (1999)
39. Golub ES, Green DR. Immunology: A Synthesis. Sinauer Associates, Sunderland, MA, USA. p. 531 (1991)
40. Roitt IM, Delves PJ. Essential Immunology. Blackwell Scientific Publications, Oxford, UK. pp. 37-47 (2001)
41. Dankwardt A. Immunochemical Assays in Pesticide Analysis. Sension GmbH, Augsburg, Germany. pp. 1-16 (2006)
42. NAQS. Annual Report About Safe Agricultural Products for Pesticide Data Program. National Agricultural Products Quality management Service (NAQS). Seoul, Korea. pp. 5-6 (2005-2006)
43. Paul J, Goulet G, Ricardo FA. Distinguishing individual vibrational fingerprints: Single-molecule surface-enhanced resonance raman scattering from one-to-one binary mixtures in langmuir-blodgett monolayers. Anal. Chem. 79: 2728-2734 (2007)
44. David W. The Immunoassay Handbook. 5th ed. Elsevier Press, Oxford, UK. pp. 286-287 (2005)
45. Masuda T, Yasumoto K, Kiatabatake N. Monitoring the irradiation-induced conformational changes of ovalbumin by using monoclonal antibodies and surface plasmon resonance. Biosci. Biotech. Bioch. 64: 710-716 (2000)
46. Markgren PO, Schaal W, Hämäläinen M, Karlén A, Hallberg A, Samuelsson B, Danielson UH. Relationships between structure and interaction kinetics for HIV-1 protease inhibitors. J. Med. Chem. 45: 5430-5439 (2002)
47. Nordin H, Jungnelius M, Karlsson R, Karlsson O. Kinetic studies of small molecule interactions with protein kinases using biosensor technology. Anal. Biochem. 340: 359-368 (2005)
48. Homola J. Surface Plasmon Resonance-based Sensors. Springer Berlin, Heidelberg, German. pp. 1221-1222 (2006)
49. Xiaoping H, Daniel JB. Influence of Au particles on the photocurrent of TiO2 films. J. Electroceram. 16: 1385-3449 (2006)
50. Quinn JG, O'Neill S, Doyle A, McAtamney C, Diamond D, MacCraith BD, O'Kennedy R. Development and application of surface plasmon resonance-based biosensors for the detection of cell–ligand interactions. Anal. Biochem. 281: 135-143 (2000)
51. Chegel VI, Shirshov YM, Piletskaya EV, Piletsky SA. Surface plasmon resonance sensor for pesticide detection. Sensor Actuat. B-Chem. 48: 456-460 (1998)
52. KFDA. MRLs for Pesticides in Foods. Korea Food & Drug Administration (KFDA), Seoul, Korea. pp. 37-114 (2005)
53. Tamura Y, Nagayama T, Takano I, Kobayashi M, Tateishi Y, Kimura N, Kitayama K, Ito M, Saito K. Survey of Pesticide Residues in Imported Crops (Organophosphorus and Organonitrogen Pesticides). Tokyo Metropolitan Research Laboratory of Public Health, Tokyo, Japan. pp. 107-111 (2001)